


Letters

Self-Decoupled and Integrated Coils for Modular Multitransmitter Wireless Power Transfer Systems

Prasad Jayathurathnage , Member, IEEE, Yining Liu , and Jorma Kyyrä , Member, IEEE

Abstract—The use of multiple transmitters (Tx) has been an attractive solution for enabling free-positioning wireless power transfer (WPT) in a large area. One of the key challenges in such multi-Tx WPT systems is the cross-coupling between Tx coils. This letter proposes a compact self-decoupled Tx coil solution for multi-Tx WPT systems. The measured cross-coupling between Tx coils has been reduced by 95% compared with conventional coil designs. In addition, an integration method for a compensation inductor with the main Tx coil is proposed. Therefore, the coil design proposed in this letter facilitates creation of fully modular and scalable Tx coils for multi-Tx WPT systems. The proposed designs are experimentally verified in a laboratory prototype.

Index Terms—Integrated coil, multitransmitter wireless power, self-decoupled coils.

I. INTRODUCTION

WIRELESS power transfer (WPT) with multiple transmitters (Tx) and receivers (Rx) has been increasingly discussed in the literature [1]–[3]. The use of multi-Tx WPT facilitates uninterrupted wireless charging in a large area or along a long track, which enables next generation wireless charging in many application domains, including charging of electrical vehicles [1], mobile robots [2], drones, kitchen appliances [3], and consumer electronics devices. In most of these WPT applications, it is desirable to have a WPT-enabled area equipped with multiple Tx, as shown in Fig. 1.

One of the key challenges in the multi-Tx WPT systems is the cross-coupling between closely spaced Tx coils [4]–[6], which may give rise to multiple unwanted issues, such as cross power transfer between Tx coils, compromised resonance conditions, excitation of reactive currents, and affecting soft switching condition of the power converters [7]. The use of overlapped coils

Manuscript received 7 April 2022; revised 10 May 2022; accepted 28 May 2022. Date of publication 10 June 2022; date of current version 26 July 2022. This work was supported in part by the Academy of Finland Postdoctoral Researcher under Grant 333479; and in part by the Business Finland Research-to-business under Grant 1527/31/2020. (Corresponding author: Prasad Jayathurathnage.)

Prasad Jayathurathnage is with the Aalto University, 00076 Aalto, Finland (e-mail: prasadku001@e.ntu.edu.sg).

Yining Liu is with the Department of Electronics and Nanoengineering, Aalto University, 00076 Aalto, Finland (e-mail: yining-liu@outlook.com).

Jorma Kyyrä is with the Electrical Engineering Department, Aalto University, FI-00076 Espoo, Finland (e-mail: jorma.kyyra@aalto.fi).

Color versions of one or more figures in this article are available at <https://doi.org/10.1109/TPEL.2022.3181508>.

Digital Object Identifier 10.1109/TPEL.2022.3181508

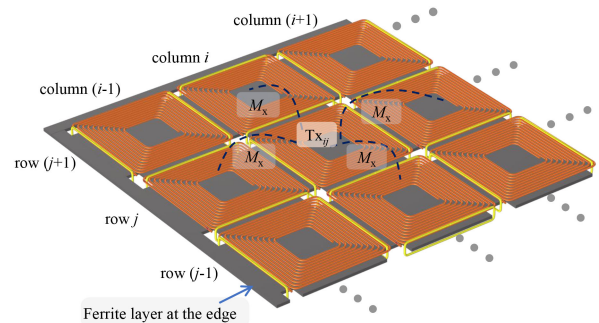


Fig. 1. Tx coil layout of a multi-Tx WPT system with the proposed coil structure.

may help to realize small cross-coupling in air-core coils [8]; however, this solution limits the design freedom as the coil positions need to be fixed. Moreover, it is not possible to fully eliminate cross-coupling between WPT coils with ferrite cores by overlapping the adjacent coils. On the other hand, most of the high-power WPT applications working at sub-kHz frequencies require coils with the ferrite material cores. Therefore, the cross-coupling between ferrite core coils is a challenging issue to solve. Recently, the use of coupled inductors connected in series with Tx was proposed to compensate the cross-coupling by introducing an additional mutual inductance with the equal magnitude and opposite sign to the cross-coupling mutual inductance [2], [6]. However, if we have a multi-Tx grid with $n \times m$ Tx, we need $[2mn - (m + n)]$ coupled inductors to compensate the cross-coupling between adjacent Tx coils, which would result in a very complex and impractical wiring. In this letter, we propose a self-decoupled WPT coil for multi-Tx WPT systems unleashing the full design freedom of large area WPT systems.

In addition, high-order compensation networks with additional inductors and/or capacitors have been proposed to achieve certain characteristics of WPT systems. For example, an LCC compensation topology at the Tx-side facilitates constant-current-driven Tx coils, which is preferred for multi-Tx WPT systems. However, a critical concern with high-order compensation networks is that the additional inductors require extra space, which limits the scalability and modularity of multiple Tx devices, and can also increase the cost of the system. To solve this issue, an integration method for the compensation

inductor was proposed in [9] for DD-type Tx coils. However, such design is not applicable for other coil shapes, such as square-shaped spiral coils; moreover, it would not be a feasible solution for multi-Tx WPT systems due to possible couplings between adjacent coils and the Rx coils. Therefore, this letter proposes a method to integrate compensation inductors within the same self-decoupled coils. The coil design introduced in this letter includes the following.

- 1) A main WPT coil that creates the WPT link with the Rx.
- 2) A set of auxiliary coils connected in series with the main WPT coil that cancel out the cross-coupling between adjacent coils.
- 3) A compensation inductor that facilitates the use of high-order compensation networks.

The coils of all three types are integrated into a single block; thus, the proposed coil structure allows fully integrated, self-decoupled, and modular solution for multi-Tx WPT systems with high-order compensation topologies.

II. PROPOSED COIL TOPOLOGY

A. Effect of Cross-Coupling Between Tx's

A Tx coil layout of a multi-Tx WPT system is shown in Fig. 1, where multiple Tx's are positioned with a grid-like arrangement. Depending on the Rx position, the Tx's need to be either activated with an ac voltage source as input, or deactivated by a short-circuited input [10]. When there is a ferrite layer under the Tx coils, mutual inductance between adjacent Tx coils is inevitable. In particular, the Tx coils facing each other can have significantly high cross-coupling compared to the ones along the diagonal directions. The cross-coupling between Tx coils causes an energy exchange between Tx's, which affects the performance and operation of the multi-Tx WPT system. These effects of cross-coupling can be evaluated by analyzing the Tx-side currents. The equivalent circuit analysis is used to derive the system equations as

$$V_s = j\omega_0 L_f I_{f,ij} + \frac{I_{f,ij} - I_{Tx,ij}}{j\omega_0 C_f} \quad (1)$$

$$0 = \left(j\omega_0 L_{Tx} + \frac{1}{j\omega_0 C_{Tx}} + R_{Tx} \right) I_{Tx,ij} - \frac{I_{f,ij} - I_{Tx,ij}}{j\omega_0 C_f} + j\omega_0 M_{ij} I_{Rx} + \sum j\omega_0 M_{xij,kl} I_{Tx,kl} \quad (2)$$

$$0 = \left(j\omega_0 L_{Rx} + \frac{1}{j\omega_0 C_{Rx}} + R_{Rx} + R_L \right) I_{Rx} + \sum j\omega_0 M_{ij} I_{Tx,ij} \quad (3)$$

where ω_0 is the working frequency, V_s is the fundamental component of the inverter output voltage, L_f is the inductance of the compensation inductor, C_f is the parallel branch capacitance, C_{Tx} is the series branch capacitance in the LCC network, M_{ij} is the mutual inductance between Rx and Tx_{ij} , i.e., the Tx coil at row i and column j , and $M_{xij,kl}$ represents the cross-coupling mutual inductance between Tx's, i.e., Tx_{ij} and Tx_{kl} , where $k, l \neq ij$. All the variables are indicated in Fig. 2.

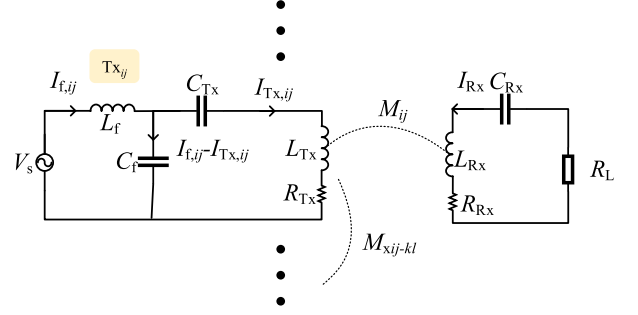


Fig. 2. Equivalent circuit of LCC-S compensated multi-Tx WPT system.

Considering the ideal lossless case, the current through the compensation inductor $I_{f,ij}$ (which is the same as the inverter output current of the active Tx) is affected by the mutual inductances between Tx's as

$$I_{f,ij} = \frac{M_{\text{sum}} M_{ij}}{L_f^2} \frac{V_s}{R_L} + j \frac{V_s}{\omega_0 L_f^2} \sum M_{xij,kl} \quad (4)$$

where M_{sum} is the sum of mutual inductances between all the active Tx coils and the Rx, which can be defined as $M_{\text{sum}} = \sum_{e \in \forall i,j} |M_{ij}|$ [2]. The sum of all mutual inductances between coil Tx_{ij} and all the other active Tx's is given by $\sum M_{xij,kl}$. We can notice from (4) that there is an introduction of reactive component to $I_{f,ij}$ due to cross-coupling between Tx's. In case of an active Tx coil, this reactive current introduces a capacitive input impedance to the full-bridge converter, which affects the soft switching condition and increases losses in the inverter. Similarly, the currents flowing through compensation inductors in inactive coils are also increased due to the effect of cross-coupling, which leads to higher losses in compensation inductor.

Besides, the abovementioned analytical derivations assume that all the compensation circuits are perfectly tuned to the desired resonance condition. However, tuning disparities are inevitable in practical implementations, which can further worsen the effects of cross-coupling. Therefore, it is clear that the cross-coupling between adjacent Tx coils needs to be mitigated in multi-Tx WPT systems. The cross-coupling between nonadjacent Tx coils are typically negligibly small; therefore, it is not necessary to take them into account. The proposed self-decoupled Tx coil consists of integrated auxiliary coils that perform the same role as cross-coupling compensation inductors. The detailed theory of the cross-coupling compensation using coupled inductors was presented in [6].

B. Proposed Self-Decoupled Coil

The proposed Tx coil structure, as shown in Fig. 3, consists of the following three types of coils integrated together.

- 1) The main WPT coil wound on top of a ferrite plate (represented in orange in Fig. 3).
- 2) Two auxiliary coils that are connected in series with the main WPT coil, but wound around the ferrite plate at two opposite sides (represented in yellow in Fig. 3).
- 3) A DD-type coil at the back-side of the ferrite plate to realize the compensation inductor (represented in green in Fig. 3).

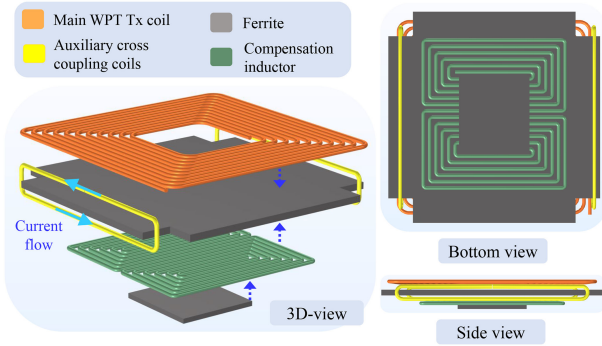


Fig. 3. Illustration of the proposed coil design. The main WPT coil and auxiliary coils are connected in series with the indicated current flow directions.

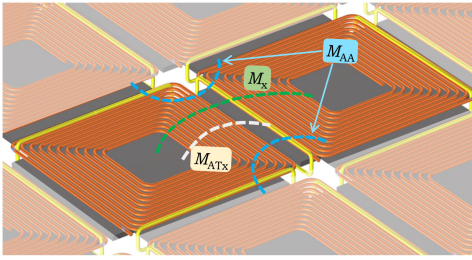


Fig. 4. Dominating coupling effects between two adjacent Tx blocks.

Compared to the conventional Tx coil structure with only a spiral main WPT coil, the proposed structure integrates two types of coils for decoupling and compensation together with the main coil. Such integration gets rid of individual decoupling inductors and compensation inductors, makes the coil structure more compact and more easily expandable for multi-Tx systems.

The auxiliary coils are connected in series with the main Tx coil, so that the current flow of the auxiliary coil branch and the main coil branch are in the opposite directions (shown in blue arrows in Fig. 3). There are two auxiliary coils connected with each Tx coil at the opposite sides. Multiple coils are arranged in such a way that the coil face with the auxiliary coil is placed next to a face without an auxiliary coil in the adjacent Tx coil, as shown in Fig. 1. This multi-Tx arrangement with auxiliary coils introduces additional coupling between auxiliary coils and the main WPT coils.

Considering any pair of two neighboring blocks, the following coupling effects are dominating (see Fig. 4).

- 1) Cross-coupling between the main Tx coils.
- 2) Coupling between two auxiliary coils of one block to one of the auxiliary coils of the other block.
- 3) Coupling between one auxiliary coil of one block and the main WPT coil of the other block.

The latter two have the opposite sign compared to the first one. The total mutual inductance between two adjacent Txs M'_x is the sum of three mutual inductances measuring these three types of coupling

$$M'_x = M_x - M_{ATx} - M_{AA} \quad (5)$$

where M_{ATx} is the mutual inductance between the auxiliary coil and its neighboring main WPT coil and M_{AA} is the mutual

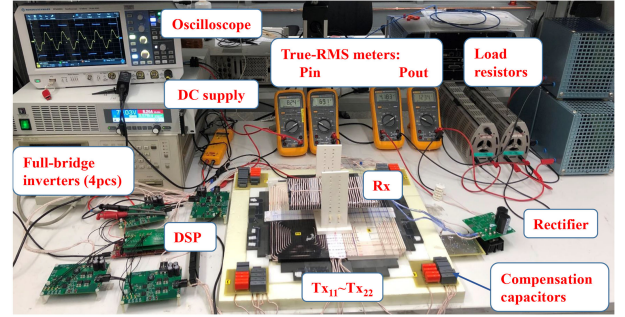


Fig. 5. Experimental setup.

inductance between two sets of auxiliary coils located on different Txs. In order to nullify the total cross-coupling M'_x , we can easily engineer the number of turns and the cross-section area of the auxiliary coils to ensure that $M'_x \approx 0$. At the edge of the whole Tx pad, a small ferrite layer is included to facilitate coupling between auxiliary coils at the edge.

C. Integration of the Compensation Inductor

In the following, in case of an *LCC*-compensated Tx, the compensation inductor is also integrated with the proposed coil structure. The compensation inductor is constructed using a DD-type coil placed at the back-side of the Tx coil, as shown in Fig. 3. Ferrite layers are used on both sides of the compensation inductor, so that the bipolar flux generated by the DD-type coil is confined to the Tx coil structure with low leakage flux. Due to the oppositely wound coils in the DD-type coil, the compensation inductor is naturally decoupled from the main WPT coil and the auxiliary coils. The desired value of the compensation inductor can easily be achieved by optimizing the coil parameters, such as the width, length, number of turns, and the size of the bottom ferrite plate.

Therefore, coils of the proposed design can be used as modular and fully integrated coils for multi-Tx WPT systems. In addition, the proposed methods for decoupling of multiple coils and integration of the compensation inductor can be used independently, depending on the application requirements. For example, decoupled coils can be used with series-compensated WPT without compensation inductors, or the integrated compensation inductor can be useful in case of a single Tx/Rx with *LCC* compensation. The proposed modular design can pave the way to realization of *WPT tiles* where whole WPT Txs together with compensation capacitors and power converters are integrated into single unit as a “tile”.

III. EXPERIMENTAL VERIFICATION

A. Experimental Setup

The proposed coil is constructed and experimentally verified in a laboratory prototype of a four-Tx WPT system. The experimental setup is shown in Fig. 5. The parameters of the constructed coils and the WPT prototype are given in Table I. The *LCC*-series compensation topology is selected for the experimental demonstration of the integrated inductor. These choices

TABLE I
SYSTEM SPECIFICATIONS AND THE COIL PARAMETERS

System Specifications					
$f_0 = \omega_0/(2\pi)$	85 kHz	Input voltage V_{DC}	70 V		
Distance z_{Rx}	55 mm	Load resistance R_L	30 Ω		
Coil Parameters					
	Length	Width	Height	Turns	Inductance
Tx	15 cm	15 cm	—	10	24.4 μH
L_f	10 cm	10 cm	—	6	17.1 μH
Rx	20 cm	10 cm	0.5 cm	40	285.7 μH

of coil dimensions and number of turns are selected in line with the prototype presented in [2] for a mobile robot charging application; however, the proposed approach can be freely applied with any other coil dimensions.

For the Rx coil, a flux pipe coil is used where the turns are wound around a ferrite block [2]. The detailed design of such Rx coils and the activation pattern of the Tx coils were discussed in [2]. It should be noted that if we consider the coupling with a Rx, the field created by the proposed Tx structure is almost identical to the usual spiral coil because the “main WPT Tx coil” (see Fig. 3), which contributes to coupling with the Rx, is just a spiral coil (auxiliary windings does not create a field towards Rx side). Therefore, the proposed Tx structure will work in the same way for other types of Rx, for example, DD-type [11] or spiral-type Rx [12]. In case of having a flux pipe or DD-type Rx coil, currents of adjacent Tx coils should be out of phase. On the other hand, if a spiral-type Rx is used, the Tx coils need to be activated with in-phase currents.

Supplied by four separate full-bridge inverters with the digital signal processor (DSP) control, the four Tx coils are controlled to have currents flowing in opposite directions between rows 1 and 2. Such operation creates magnetic fields in opposite directions to couple with the flux pipe-type Rx [2]. All the Tx and Rx coils are tuned to the designed operating frequency f_0 together with compensation networks [9]. A diode bridge rectifier is used with a passive resistor bank at the Rx-side. A DSP, *TMS320F28379*, is used to generate control signals for inverters. The waveforms are observed using an oscilloscope, the input and output dc powers are measured using industrial grade true root mean square (rms) meters (*FLUKE 28-II*).

B. Coil Measurement

The measurement results of the WPT coils, including inductances, mutual coupling inductances, and mutual inductances with Rx, are compared with those for the classical coil design. First, the cross-coupling mutual inductances between Tx coils are compared in Fig. 7 for two cases: 1) between classical spiral-shaped Tx coils; and 2) between the proposed self-decoupled Tx coils with the same configuration in the main WPT coils.

A guideline for auxiliary coils design is then proposed. The first step is to estimate the cross-coupling between adjacent main WPT coils through measurements or simulations. Next, by changing the number of turns n and surface area $A = l \times h$ of the auxiliary coils, the sum of M_{ATx} and M_{AA} can be adjusted

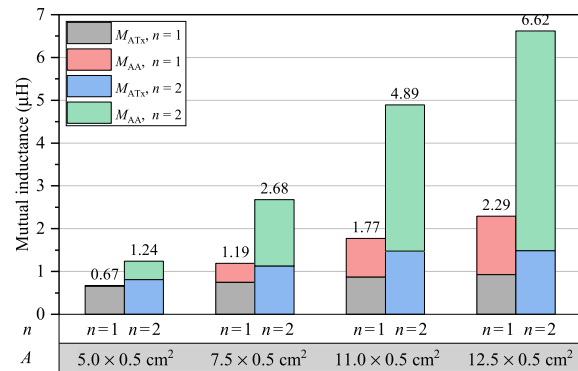


Fig. 6. Variation of the compensation coupling against design parameters, the number of turns n , and surface area $A = l \times h$ of the auxiliary coils.

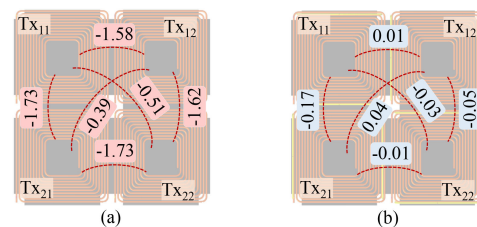


Fig. 7. Results of cross-coupling mutual inductance measurement (μH) between Tx coils with the following. (a) Classical Tx structure without cross-coupling compensation. (b) Proposed self-decoupled Tx structure.

to compensate the existing cross-coupling, according to (5). Limited by the increase in coil series resistance and ferrite core saturation, the number of turns and surface area of the auxiliary coils are adjusted between $n = 1 \sim 2$ and $A = 5.0 \times 0.5 \sim 12.5 \times 0.5 (\text{cm}^2)$. The variation of the compensation coupling against design parameters is shown in Fig. 6. The sum of each stacked column indicates the total compensation mutual inductance brought by auxiliary coils (i.e., $M_{ATx} + M_{AA}$), which can be adjusted between 0.67 and 6.62 μH for the given Tx structure. It is shown that n has a very strong effect on compensation, while the length l can be adjusted continuously and chosen as any value within the given range to compensate M_x . Therefore, the above-mentioned design method for the selection of proper parameters for the auxiliary coil is also applicable to Tx coils with different dimensions. As a result, the coil parameter for the Tx coils in Fig. 7(a) is chosen as $n = 1$ and $A = 11.0 \times 0.5 (\text{cm}^2)$.

The self-decoupled coils with designed auxiliary turns and related inductances are shown in Fig. 7(b). Considering the original mutual inductance with negative signs in Fig. 7(a), the signs of decoupled results in Fig. 7(b) indicate the undercompensated (with negative signs being the same as in the original measurement) or overcompensated (with positive signs that are opposite to those in the original measurements) situations. We see that the residual cross-coupling effects are very small, since the absolute values of the decoupled results clearly show that the dominate cross-couplings between the adjacent Tx coils are reduced to lower than 10% of the original cross-coupling inductances of spiral Tx coils. Comparing the total cross-coupling mutual inductances $\sum M_{xij}$ between these two implementations, the proposed coil structure provides a reduction greater than 95%.

TABLE II
CROSS-COUPLING MUTUAL INDUCTANCE MEASUREMENT (μH)

Cross-coupling		T_{x11}	T_{x12}	T_{x21}	T_{x22}
ΣM_{Tx}	Original	-3.820	-3.589	-3.867	-3.856
	decoupled	-0.185	-0.003	-0.088	-0.140
M_{Tx-Lf}		0.017	0.070	0.015	0.035

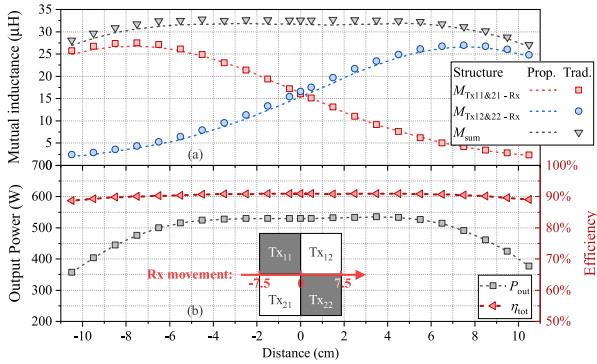


Fig. 8. (a) Mutual inductance between the Tx and Rx. (b) Output power and system efficiency against movement.

The cross-coupling between the integrated compensation inductor L_f and the corresponding main Tx coil is also verified to be negligibly small, as seen from the measured mutual inductances in Table II.

In the following, the mutual inductances between Rx and Txs are measured at different positions during Rx movement along the middle line between the two rows of Tx coils, as shown in Fig. 8(a).

Distance 0 cm corresponds to the middle of two Tx columns. Since the auxiliary coils have opposite direction to the main coil, the mutual inductance between Txs and Rx will be reduced. To estimate this reduction effect, $M_{sum} = M_{Tx11\&21-Rx} + M_{Tx12\&22-Rx}$ are compared between the original and the proposed decoupled structures. Along the entire Rx movement range, the proposed fully integrated coil structure exhibits a very similar mutual inductance profile, as compared to the traditional structure with square-shaped spiral coils. The reduction of M_{sum} has the maximum ratio of only 3.5% at the two edge positions, and the minimum ratio of 2.3% in the middle. Therefore, the WPT performance, including efficiency and output power, will remain almost unaffected by a slight reduction of mutual inductance of the proposed self-decoupled coils.

C. System-Level Measurement

Moving forward, the proposed Tx coils are then implemented into an LCC-series compensated WPT system. The output power and efficiencies are measured during the same Rx movement along the middle line of two Tx rows. The results in Fig. 8(b) demonstrate nearly constant system dc-to-dc efficiency around 90% against the movement. The WPT system is able to provide output power higher than 500 W at the optimal position.

Furthermore, the advantages of fully decoupled Txs can be revealed observing the current through the compensation inductor

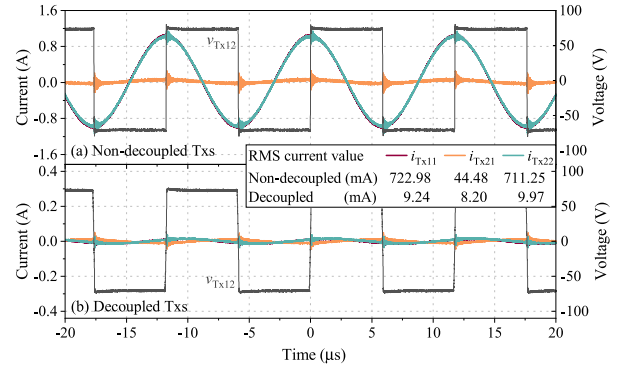


Fig. 9. Active Tx input voltage and inactive Tx current when the Tx coils are (a) not decoupled; and (b) fully decoupled.

of inactive Txs when Rx is not present. In this case, the real part of current $I_{f,ij}$ is brought to zero due to zero mutual inductance with the Rx M_{ij} , refer to (4). If we activate only one of the Tx coils (e.g., T_{x12}), while keeping the other three coils inactive, the reactive part of $I_{f,ij}$ is affected only by cross-coupling between T_{xij} and T_{x12} , following (4). As shown in Fig. 9(b), the total current of each inactive Tx has the rms value smaller than 10 mA since $\Sigma M_{xij} \approx 0$. Then, we manually create some additional cross-coupling between every two adjacent coils by adding a piece of 5×5 cm ferrite slab at four boundaries, which results in a similar cross-coupling as in conventional square-shaped spiral coils. The input current of two adjacent inactive coils in Fig. 9(a): 1) $I_{f,11}$; and 2) $I_{f,22}$, increases to approximately 722-mA rms at the measured mutual inductance of $1.72 \mu\text{H}$. The input current in the diagonal coil $I_{f,21}$ also increases a bit to 44-mA rms due to the increased ΣM_{x21} of $0.3 \mu\text{H}$. These results clearly verify that the effects of cross-coupling have been fully eliminated with the proposed coil design.

IV. CONCLUSION

This letter proposed a novel coil design for realizing self-decoupled modular Tx coils for multi-Tx WPT systems and a new integration method for compensation inductors to the main WPT coil in high-order compensation networks. This coil design can be used as a modular building block for multi-Tx WPT systems. The proposed self-decoupled coils include auxiliary coils to compensate cross-coupling between Tx coils. The experimental results showed more than 95% reduction of cross-coupling between Txs as compared to the classical square-shaped spiral coils. In addition, the compensation inductor was also integrated with the proposed Tx coil. A laboratory prototype with the proposed coil design was built to verify the efficacy of the introduced design. We conclude that the proposed coil design can be used as a modular and scalable building block of multi-Tx WPT systems.

ACKNOWLEDGMENT

The authors would like to thank Professor Sergei Tretyakov for the guidance and useful discussions.

REFERENCES

- [1] C. C. Mi, G. Buja, S. Y. Choi, and C. T. Rim, "Modern advances in wireless power transfer systems for roadway powered electric vehicles," *IEEE Trans. Ind. Electron.*, vol. 63, no. 10, pp. 6533–6545, Oct. 2016.
- [2] S. Al Mahmud, I. A. Panhwar, and P. K. S. Jayathurathnage, "Large-area free-positioning wireless power transfer to movable receivers," *IEEE Trans. Ind. Electron.*, to be published, doi: [10.1109/TIE.2022.3144591](https://doi.org/10.1109/TIE.2022.3144591).
- [3] S. Nutwong, A. Sangswang, S. Naetiladdanon, and E. Mujjalinvimut, "A novel output power control of wireless powering kitchen appliance system with free-positioning feature," *Energies*, vol. 11, no. 7, 2018, Art. no. 1671.
- [4] D. Ahn and S. Hong, "Effect of coupling between multiple transmitters or multiple receivers on wireless power transfer," *IEEE Trans. Ind. Electron.*, vol. 60, no. 7, pp. 2602–2613, Jul. 2013.
- [5] G. Yang *et al.*, "Interoperability improvement for wireless electric vehicle charging system using adaptive phase-control transmitter," *IEEE Access*, vol. 7, pp. 41365–41379, 2019.
- [6] F. Farajizadeh, D. M. Vilathgamuwa, D. Jovanovic, P. Jayathurathnage, G. Ledwich, and U. Madawala, "Expandable N-legged converter to drive closely spaced multitransmitter wireless power transfer systems for dynamic charging," *IEEE Trans. Power Electron.*, vol. 35, no. 4, pp. 3794–3806, Apr. 2020.
- [7] C. Zhu, W. Zhong, and D. Xu, "Decoupling control of modular WPT systems," in *Proc. IEEE Appl. Power Electron. Conf. Expo.*, 2020, pp. 3125–3131.
- [8] U. Pratik, B. J. Varghese, A. Azad, and Z. Pantic, "Optimum design of decoupled concentric coils for operation in double-receiver wireless power transfer systems," *IEEE Trans. Emerg. Sel. Topics Power Electron.*, vol. 7, no. 3, pp. 1982–1998, Sep. 2019.
- [9] T. Kan, T.-D. Nguyen, J. C. White, R. K. Malhan, and C. C. Mi, "A new integration method for an electric vehicle wireless charging system using LCC compensation topology: Analysis and design," *IEEE Trans. Power Electron.*, vol. 32, no. 2, pp. 1638–1650, Feb. 2017.
- [10] W. Kim, "Efficient deactivation of unused LCC inverter for multiple transmitter wireless power transfer," *IET Power Electron.*, vol. 12, no. 10, pp. 72–82, Jan. 2019.
- [11] S. Zhou and C. C. Mi, "Multi-paralleled LCC reactive power compensation networks and their tuning method for electric vehicle dynamic wireless charging," *IEEE Trans. Ind. Electron.*, vol. 63, no. 10, pp. 6546–6556, Oct. 2016.
- [12] F. Lu, H. Zhang, H. Hofmann, and C. C. Mi, "A dynamic charging system with reduced output power pulsation for electric vehicles," *IEEE Trans. Ind. Electron.*, vol. 63, no. 10, pp. 6580–6590, Oct. 2016.